Journal of Materials Chemistry B

PAPER

View Article Online
View Journal

Cite this: DOI: 10.1039/c5tb00099h

Conducting polymer electrodes for auditory brainstem implants

Amélie A. Guex,[a] Nicolas Vachicouras,[a] Ariel Edward Hight,[b] M. Christian Brown,[b] Daniel J. Lee[b] and Stéphanie P. Lacour*[a]

Received 15th January 2015
Accepted 12th February 2015

DOI: 10.1039/c5tb00099h

www.rsc.org/MaterialsB

The auditory brainstem implant (ABI) restores hearing in patients with damaged auditory nerves. One of the main ideas to improve the efficacy of ABIs is to increase spatial specificity of stimulation, in order to minimize extra-auditory side-effects and to maximize the tonotopy of stimulation. This study reports on the development of a microfabricated conformable electrode array with small (100 μm diameter) electrode sites. The latter are coated with a conducting polymer, PEDOT:PSS, to offer high charge injection properties and to safely stimulate the auditory system with small stimulation sites. We report on the design and fabrication of the polymer implant, and characterize the coatings in physiological conditions *in vitro* and under mechanical deformation. We characterize the coating electrochemically and during bending tests. We present a proof of principle experiment where the auditory system is efficiently activated by the flexible polymeric interface in a rat model *in vivo*. These results demonstrate the potential of using conducting polymer coatings on small electrode sites for electrochemically safe and efficient stimulation of the central auditory system.

1. Introduction

Auditory brainstem implants (ABI) are an alternative hearing strategy for patients suffering from sensorineural hearing loss who cannot benefit from cochlear implants (CI) because of a disconnection between the peripheral and central auditory systems. ABIs target the cochlear nucleus (CN), the first processing station of the central auditory system, located at the dorsolateral surface of the brainstem.[1] ABIs provide auditory sensations and help with lip reading for most patients. However, speech hearing performance is relatively poor compared to the high outcomes obtained in most patients with CIs; in spare cases, audiologic outcomes of ABI patients are excellent.[2] The modest efficacy of auditory brainstem stimulation may be due to spread of electric current leading to broad activation of neurons along the tonotopic axis of the CN and stimulation of extra-auditory neurons, causing side-effects. Based on this hypothesis, improving the spatial specificity of stimulation is a route for improving the ABI clinical outcomes.

Clinical ABIs consist of a rigid 0.6 mm thick pad hosting 15 to 21 platinum electrode sites with a diameter in the 550 μm to 700 μm range embedded in silicone elastomer. The array is surgically inserted at the surface of the CN. ABIs are often found too rigid to conform the curvilinear surface of the CN thereby preventing efficient transduction of the electrical stimulation in the CN. Recent advances in flexible bioelectronics provide alternative materials and designs for implantable neural interfaces. In this paper, we propose using flexible polymers to engineer and manufacture a conformable ABI. A compliant substrate may also decrease the mechanical mismatch between the implant and the tissue, and minimize chronic inflammation.[3,4] The proximity of the stimulation sites to the targeted neurons combined with limited implant encapsulation may also decrease stimulation current thresholds and improve its efficiency. Spatial specificity of stimulation may also be improved by modifying the geometry and arrangement of the stimulation sites, *e.g.* higher electrode density and smaller electrode diameter. A major limitation to reducing electrode area is the associated higher electrode impedance and lower safely injectable charge during electrical stimulation. This reduces the effective dynamic range of current levels between stimulation and damage thresholds. Many potential solutions have been proposed to improve the electrode–electrolyte interface by lowering the electrode impedance and increasing their charge injection capacity (CIC). This may be achieved by increasing the surface roughness of the electrode. The electrode effective surface area is then larger than its geometrical surface area and the charge injection is more efficient.

Among these potential solutions, conducting polymers (mainly polypyrrole, PPy, and poly(3,4-ethylenedioxythiophene), PEDOT) have gained substantial interest over the past ten years for recording and stimulation electrodes.[5] Although PPy

[a]*Center for Neuroprosthetics, Ecole Polytechnique Fédérale de Lausanne, Lausanne, Switzerland. E-mail: stephanie.lacour@epfl.ch; Fax: +41 21 693 78 20; Tel: +41 21 693 11 81*

[b]*Eaton-Peabody Laboratories and Department of Otolaryngology – Head and Neck Surgery, Massachusetts Eye and Ear Infirmary, Department of Otology and Laryngology, Harvard Medical School, Boston, Massachusetts, USA*

properties have been extensively studied in the literature, PEDOT is generally preferred for biomedical applications because of its higher electrochemical stability.[6] The surface of a PEDOT film is usually rough; its hybrid ionic–electronic charge transfer properties allow for very efficient charge transfer to the biological medium.[5,7] Moreover, PEDOT coatings under stimulation conditions show excellent biocompatibility, with good neuronal adhesion and growth *in vitro*[8] and *in vivo*.[9] *In vivo* PEDOT electropolymerization has also been demonstrated, with good electrical performance and no impairment of function.[10] PEDOT has also been used to improve electrode properties for auditory system applications. In the cochlea, PEDOT was integrated with a functionalized alginate hydrogel for low impedance electrodes with concurrent drug delivery.[11] PEDOT-coated microelectrodes provided efficient microstimulation of the auditory cortex.[12] PEDOT was also shown to improve the recording SNR of hydrogel-coated electrodes in the auditory cortex.[13] Although some studies report on a limited stability of PEDOT under repeated pulsing in chronic conditions,[14] it appears as a good alternative to metal films in an acute application aiming at improving charge transduction properties of electrode sites.

In this paper, we report on the characterization of PEDOT with doping agent PSS (polystyrene sulfonate) deposited above thin film platinum electrodes by galvanostatic electropolymerization from a solution of EDOT:PSS. Imaging and electrochemical characterization of PEDOT:PSS deposited with different charge deposition conditions are presented. The electrode array is embedded in a flexible polyimide film, and its reliability upon bending is assessed. In an acute setting, we recorded electrically evoked auditory brainstem responses (eABRs), a far-field response generated by the sequential activation of the auditory nuclei in the brainstem,[15] induced by electrical stimulation of the CN with the flexible electrode array. eABRs are a simple and non-invasive way to assess the activation of the auditory system. eABRs are also used clinically; in fact, during ABI implantation surgery, they are used to help position the implant at the surface of the CN.[2]

2. Methods

2.1. Fabrication

The electrode arrays were fabricated using standard microfabrication processes.[16,17] A sacrificial layer of Ti (5 nm)/Al (50 nm) was first deposited by evaporation on a silicon wafer. A first layer of polyimide (PI2611, HD Microsystems GmbH, Germany) was then spin-coated and cured (soft bake, 5 min at 120 °C followed by hard bake for 2 hours at 300 °C in a N_2 oven). The interconnects layer (Ti/Pt/Ti, 75/350/75 nm) was then sputtered after O_2 plasma surface activation and patterned by photolithography and RIE (reactive ion etching). A second layer of PI was subsequently spin-coated and cured. A 500 nm SiO_2 layer was next deposited and patterned to serve as an etch mask. Patterning of the SiO_2 film defines both the electrode active sites and the implant external shape. The oxide and polyimide films were etched by RIE. For thin polyimide implants (5–10 μm thick), SiO_2 masking was replaced by a thick photoresist coating. The electrode arrays were subsequently released from the wafer by anodic dissolution of the Al layer (1 V bias, in saturated NaCl solution).[16]

2.2. PEDOT:PSS preparation and electropolymerization

PEDOT:PSS was electropolymerized from a solution of EDOT (0.1% w/v) and PSS (0.2% w/v) (both purchased from Sigma Aldrich). Prior to electropolymerization, the electrodes were cleaned with UV/ozone treatment for 30 s. Electropolymerization was performed galvanostatically at 0.75 mA cm^{-2} with a platinum counter electrode and an Ag/AgCl reference electrode. PEDOT:PSS coatings were electropolymerized with different deposition charges (75–600 mC cm^{-2}) by increasing the deposition time. After electropolymerization, the devices were rinsed in dH_2O and air dried.

2.3. Electrochemical measurements

2.3.1 Electrochemical impedance spectroscopy. Electrochemical measurements were made in a 3-electrode setup with a potentiostat (Gamry ref. 600, Gamry Framework) with a large area platinum counter electrode and an Ag/AgCl reference electrode. Measurements were performed at room temperature, in PBS (pH: 7.4). Complex impedances were measured by electrochemical impedance spectroscopy (EIS), with an AC voltage of 5 mV RMS and no DC bias, between 100 Hz and 1 MHz.

2.3.2 Cyclic voltammetry. Cyclic voltammetry was performed by cycling the potential between the limits of water electrolysis (typically −0.6 to 0.8 V) at a speed of 50 mV s^{-1}. Cathodic charge storage capacity was calculated by integration of the cathodic current over one cycle of CV.

2.3.3 Voltage transients. Charge injection capacity (CIC) is defined as the maximum charge that can be injected without the potential of the interface going beyond the limits of the water window. It was measured for a particular pulse waveform and frequency by increasing the current level step by step and measuring the voltage transients. This transient is composed for each phase of several components. The initial quasi-instantaneous drop is called the ohmic drop and is due to the resistance of the circuit and solution. It was defined as the drop in potential occurring during the first 10 μs of the pulse. The potential at the interface after subtraction of the ohmic drop was used to measure CIC, the maximum charge for which the negative and positive potentials remain within the electrochemically safe window.[18]

2.4. SEM

Samples were imaged under vacuum in a Zeiss Merlin scanning electron microscope (SEM) with an accelerating potential of 0.8 kV and a current of 15 pA. Working distance was 4.1 mm and magnification was 15 000×.

2.5. Thickness measurements

Thickness of the PEDOT:PSS coatings were measured by mechanical profilometry, with a DektakCT stylus surface profiler. A force of 3 mg was used.

2.6. Bending tests

To perform bending tests, the PEDOT coated devices were bent around rods of radius of curvature ranging from 2, 1.75, 1.5, 1.25 down to 1 mm. The complex impedance spectrum of the electrodes was measured before the test and immediately after, and so on until the smallest bending radius. The coatings were also inspected with an optical microscope to detect potential cracks or delamination.

2.7. *In vivo* evaluation

All experimental procedures were performed in accordance with the National Institute of Health guidelines for the care and use of laboratory animals as well as approved animal care and use protocols at the Massachusetts Eye & Ear Infirmary, Boston, MA. Acute *in vivo* tests were performed on Sprague-Dawley rats (350–500 g) within a sound-attenuation chamber. A total of 7 animals were used for these experiments. Animals were first anesthetized with ketamine (100 mg kg^{-1}) and xylazine (20 mg kg^{-1}), and an occipital craniotomy was performed. After cerebellar aspiration, the rat dorsal brainstem was exposed and the array was placed on the surface of the CN. Stimulation was induced with charge-balanced biphasic symmetric pulses, 0.2 ms per phase, at 23 pulses per second, with alternating polarity. Four different arrays were used in total. Before re-using an array, the integrity of the electrode sites was checked by EIS. eABRs were recorded by subtracting the signals obtained from two subcutaneous stainless steel needle electrodes placed on the vertex and behind the ipsilateral pinna of the animal, with respect to a ground electrode on the back of the animal. The signal was filtered with an analog bandpass filter (30 Hz to 3 kHz) and amplified by 60 dB before A/D conversion with a sampling frequency of 25 kHz (Ithaco Model 1201, DL Instruments, Ithaca, NY). The first 10 ms of this signal following each stimulation pulse was averaged over 512 stimulus presentations and filtered with a forward and reverse bandpass Butterworth filter of order 5 between 200 Hz and 2.5 kHz.

2.8. Statistical tests

Results are expressed as mean ± standard error of the mean. Statistical significance of data was determined by an analysis of variance (ANOVA) and with a *post-hoc* Tukey–Kramer test performed with Matlab software (The Mathworks Inc., Natick, MA). A p-value was determined and significance was indicated by a value lower than 0.05.

3. Results

3.1. PEDOT:PSS electrochemical study

In the first phase of this study, we compared the electrochemical properties of the PEDOT:PSS coating at different deposition charges. Larger deposition charges generated thicker coatings (Fig. 1). The roughness of the coating surface is visible on the SEM image.

PEDOT:PSS coating induced a decrease in impedance modulus at 1 kHz of more than one order of magnitude (from 45.27 ± 2.62 kΩ for Pt to 2.6 ± 0.66 kΩ for PEDOT:PSS of 0.6 μm thickness) (Fig. 2a and b). Moreover, the phase of the impedance is close to zero over the entire range of measured frequencies, indicating a resistive behaviour associated with PEDOT:PSS charge-injection mechanism. The change of impedance between the different deposition conditions is not significant ($p > 0.05$), indicating a negligible effect of the PEDOT:PSS thickness on the impedance modulus and phase. Cathodal charge storage capacity (cCSC) measurements obtained from the CV measurements show a non significant increase in cCSC between the platinum electrode and the thinnest coating ($p > 0.05$) (Fig. 2c and d). Larger charge depositions generated a substantial and steady increase in cCSC ($p < 0.05$ for all conditions). Fig. 2e displays an example of charge injection capacity measurement with a biphasic cathodic-first pulse at 20 Hz and 0.2 ms per phase. The voltage transients following current pulses of increasing amplitudes (0.05 to 0.6 mA) before and after subtraction of the ohmic drop are plotted. Fig. 2f shows the behavior of the CIC of PEDOT:PSS-coated electrode sites with different deposition charges for 100 μm diameter electrode sites. A significant effect of the PEDOT:PSS deposition charge on CIC is obtained ($p < 0.05$). A *post-hoc* test determined that only the 75 mC cm^{-2} is significantly different from other conditions (450 and 600 mC cm^{-2}) ($p < 0.05$).

One important feature of the polyimide array is its flexibility. The PEDOT:PSS coating of the electrode sites must therefore remain intact upon bending to a radius of curvature corresponding to the estimated *in vivo* minimal bending radius, about 1.6 mm. This value was determined from a 3D reconstruction of a rat brainstem (Fig. 3a).[19] Results of the bending tests show no significant change in impedance modulus at 1 kHz of the coated electrode sites, in all deposition charge conditions ($p > 0.05$) (Fig. 3b). Furthermore, no cracks nor delamination of the coating were observed during any tested bending conditions (Fig. 3c).

3.2. Application and *in vivo* test

ABI arrays with a polyimide thickness of 8 μm were used for *in vivo* tests. With such thickness, the capillary forces are sufficient to induce a bending of the polyimide device around a wet cylindrical surface without any other external force applied.[20] A finger-like design was developed in order to further optimize the conformability of the array (Fig. 4a). In the context of this application, one desired feature is a high density of electrodes on the available 1-by-2 mm surface of the surgically exposed rat CN, in order to be able to precisely tune the stimulation position and optimize the spatial specificity of stimulation. An electrode diameter of 100 μm was selected for this purpose.

Under these conditions, PEDOT:PSS with 75 mC cm^{-2} deposition charge was selected for further testing. Indeed, the low thickness of the polyimide substrate induces mechanically challenging conditions, and coatings with higher deposition charges tend to crack and delaminate from the substrate. The coating with 75 mC cm^{-2} deposition charge is the thinnest and thus has the least induced stress in the film.

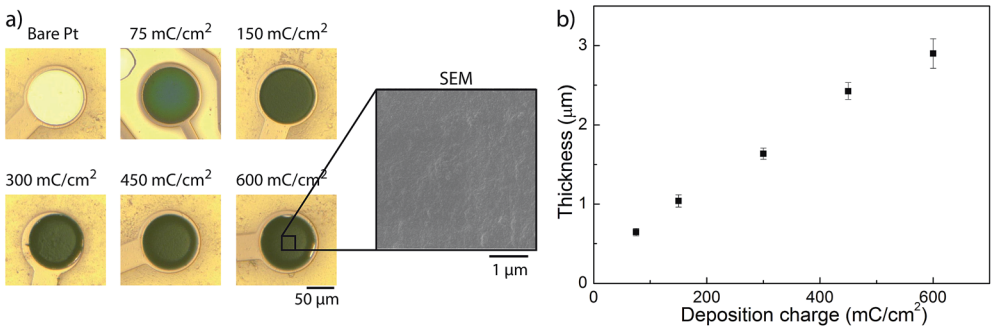

Fig. 1 (a) Optical images of PEDOT films grown with various deposition charges (in mC cm^{-2}). SEM image illustrating the surface roughness of the PEDOT:PSS coating. (b) PEDOT:PSS film thickness as a function of deposition charge ($N = 5$).

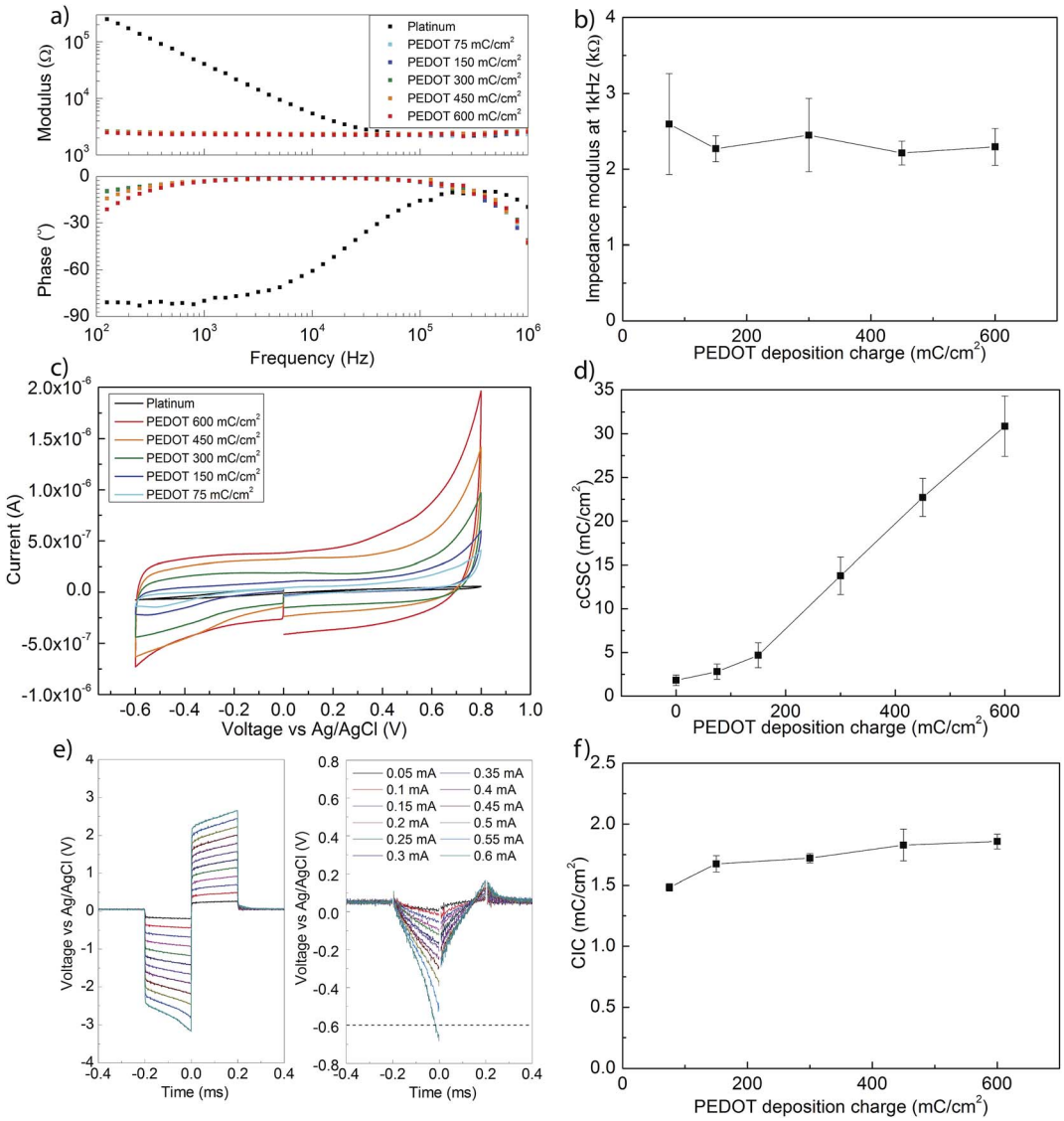

Fig. 2 (a) Electrochemical impedance spectra and (b) impedance modulus at 1 kHz following PEDOT:PSS deposition with different deposition charges on 200 µm diameter electrodes ($N = 5$). (c) Cyclic voltammograms of 200 µm diameter PEDOT:PSS coated electrodes and (d) cCSC of PEDOT:PSS films prepared with increasing deposition charges ($N = 5$). (e) Voltage transients measured during biphasic current pulses and recorded with increasing stimulation currents, before (left) and after (right) removal of the ohmic drop on 100 µm diameter electrodes. (f) Average CIC of PEDOT at different deposition charges ($N = 5$).

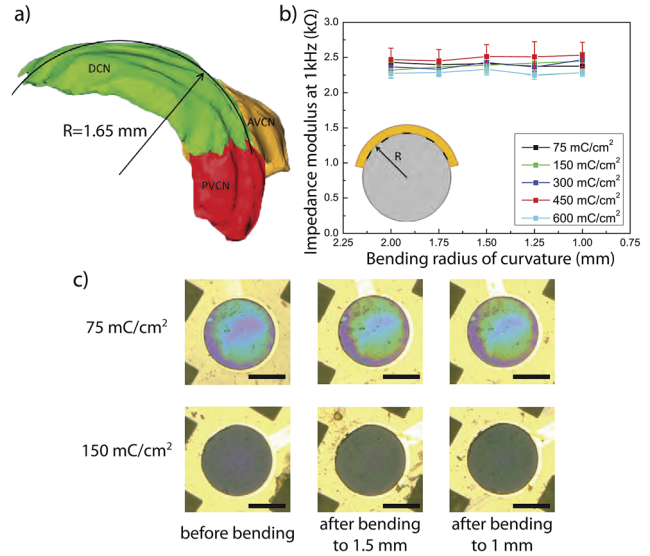

Fig. 3 (a) 3D reconstruction of a rat cochelar nucleus. The dorsal cochlear nucleus has a radius of 1.65 mm.[19] DCN: dorsal cochlear nucleus, AVCN: anteroventral cochlear nucleus, PVCN: posteroventral cochlear nucleus. (b) Impedance modulus at 1 kHz of PEDOT:PSS coated electrodes (diameter = 200 μm) after increasing compressive bending. (c) Optical images of two electrode sites before bending, after bending to 1.5 mm radius and to 1 mm radius indicating the absence of cracks or delamination of the coating. Scale bars: 50 μm.

Moreover, as mentioned in the previous section, the CIC and impedance values of the thinnest coating are very similar to the values at higher deposition charges. Choosing the thinnest coating thus guaranteed a greater mechanical stability without compromising the electrochemical properties and the safety of stimulation. A plot of the complex impedance spectrum of over 100 sites before and after coating with PEDOT:PSS at 75 mC cm^{-2} shows repeatability of PEDOT:PSS coating impedance characteristics (Fig. 4b).

Another crucial property that we tested was the array's ability to generate eABRs. Results showed that it is possible to generate eABRs with the PEDOT:PSS coated electrode array in each of the 7 tested animals. An example of eABR is shown on Fig. 5. Threshold for eABR generation is between 0.25 and 0.5 mA, and a large positive peak followed by a smaller negative peak can be seen. The amplitude of the noise was estimated to be 0.15 μV in this example. The ratio between the amplitude of the peaks and the noise is 3.89. This waveform is typical of eABRs.[2] Twenty electrode sites from 3 different arrays were analyzed after the acute *in vivo* tests to confirm integrity of the PEDOT:PSS coating. On the 20 explanted electrode sites, 19 appeared intact on the microscope while one PEDOT:PSS coating appeared delaminated and was not considered for further analysis. Electrochemical tests (EIS and CV) were subsequently performed on these 19 electrode sites. No significant change in impedance modulus at 1 kHz was observed after the *in vivo* test compared to that of the pristine electrodes (Fig. 6). Furthermore, cCSC after explantation of active (stimulated) sites and passive (non-stimulated) sites showed no significant change, indicating no loss in electroactivity of the coating due to stimulation.

4. Discussion

These results show the possible use of electropolymerized PEDOT:PSS coatings in a therapeutic application-driven study with acute *in vivo* tests. In a first phase, properties of PEDOT:PSS with different deposition charges were investigated. In a second phase, the application required thinner, more flexible polyimide substrate, which created a more mechanically challenging environment for the PEDOT:PSS coating. A 75 mC cm^{-2} deposition charge was hence selected, and proved to have electrical properties suitable for auditory brainstem stimulation. For this acute application, the PEDOT:PSS was very reliably electrodeposited and showed suitable properties in terms of size, thickness, bendability, impedance and charge injection capacity.

The electrochemical window limits are often considered to be between −0.6 and 0.8 V for platinum and −0.6 to 0.8 V or −0.9 to 0.5 V for PEDOT:PSS.[14,18] However, these limits highly depend on the conditions such as the temperature, the electrolyte composition and pH and the counter electrode material. In order to measure them on a case-by case basis, CV cycles can be performed with very wide voltage limits. The negative voltage

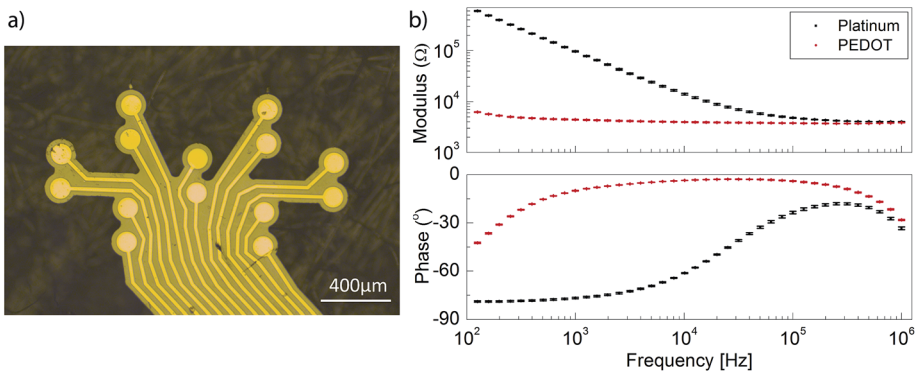

Fig. 4 (a) Picture of the electrode array fabricated on thin polyimide substrate with a finger-like shape to further increase conformability. (b) Impedance modulus and phase spectra of a bare Pt and PEDOT:PSS coated electrodes (diameter = 100 μm). The small values of the error bars for the PEDOT:PSS coated electrodes (N = 100 sites) demonstrate great repeatability of the coating.

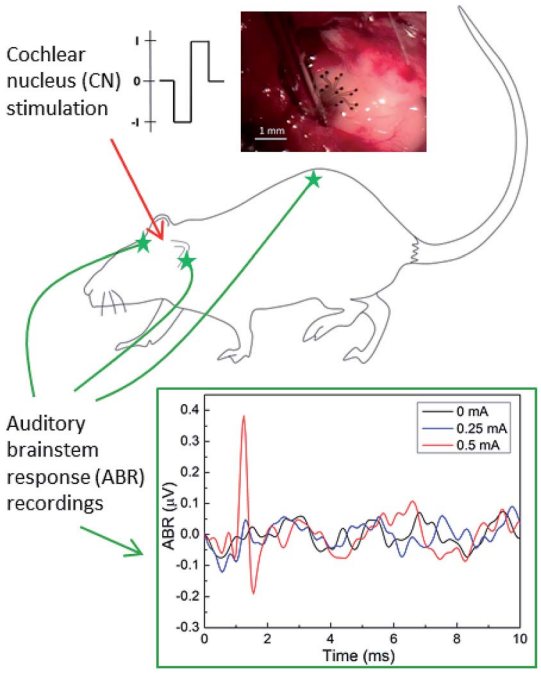

Fig. 5 Auditory brainstem responses (ABR) recorded following stimulation of the cochlear nucleus surface with the PEDOT:PSS coated electrode array. Photomicrograph shows the array in position on the exposed surface of the CN on the left side of the brainstem. Diagram shows the positions of the ABR recording electrodes.

where the current drops and the positive voltage where the current quickly rises reflect water electrolysis and are the true limits of the water window. However, water window limits determined *in vitro* for this application will still be different from *in vivo* limits. The choice was then made to measure all electrochemical properties with respect to the −0.6 to 0.8 V limits. These values are quite conservative and widely used in the literature.

The stimulation used here is electrochemically safe *in vitro* at room temperature in PBS. However, the CIC can be very different in physiological conditions, at 37 °C.[18] Moreover, the electrochemical limit is not the only safety limit to consider for chronic stimulation. There is another limit of charge density above which the chronic overstimulation of neurons induces neuronal damage, first described by McCreery and coworkers.[21,22] With 100 μm diameter electrodes and the pulse waveform used in this study, this limit corresponds to a current level of about 0.2 mA. This current is below eABR threshold during acute *in vivo* stimulation (about 0.5 mA). In order to develop a chronic stimulation model with this ABI array, the diameter would thus need to be increased. Moreover, the PEDOT:PSS coating electrodeposited on smooth platinum surface has been shown to be less stable than PEDOT:PSS or PEDOT:pTS (*para*-toluene sulfonate) electrodeposited on rough platinum for chronic applications.[14] This reduces delamination from the substrate and improves the electrochemical stability of the coating, which are currently the two main issues for developing a chronically stable coating with high charge injection capacity and small impedance. This is however beyond the scope of this paper, as the PEDOT:PSS coating is used here in an acute setup to help optimize stimulation parameters.

The particularity of the ABI application is its placement at the surface of the brainstem. Attempts have been made to develop a penetrating ABI (pABI) that is in closer proximity with the target neurons. Smaller currents were required to elicit auditory responses but overall, no significant improvements were observed compared to surface ABIs.[23] Given the higher invasiveness of pABIs and the greater difficulty to adapt their placement during surgery, an optimization of the surface approach was chosen. The properties of this implant thus need to be halfway between intracortical electrodes and surface electrodes. The former have very small exposed areas and small current thresholds due to close proximity to the target neurons but are usually associated to stronger chronic inflammation

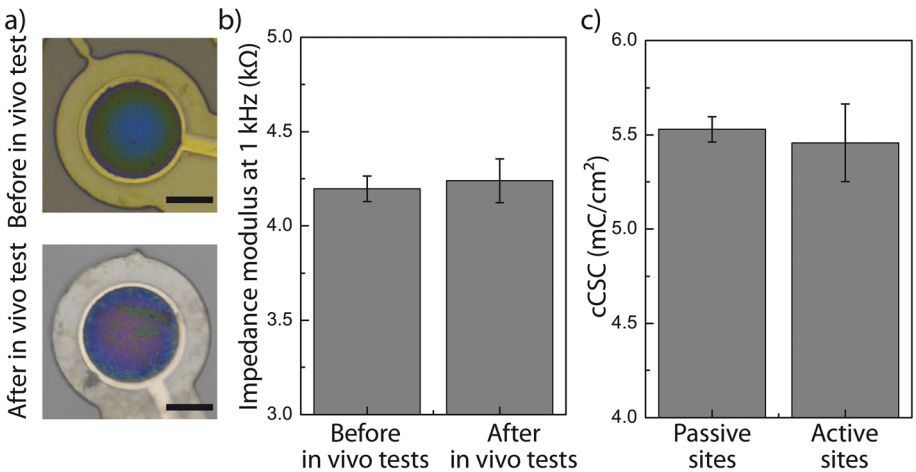

Fig. 6 (a) Optical images of PEDOT films on 100 μm diameter electrode sites before and after *in vivo* tests. Scale bars: 50 μm. (b) Impedance modulus at 1 kHz before and after *in vivo* tests showing no significant difference ($p > 0.05$, $N = 19$). (c) cCSC of passive and active sites after explantation, showing no significant difference in the electrochemical properties of the PEDOT:PSS film ($p > 0.05$, $N = 7$ for passive sites, $N = 19$ for active sites).

and high invasiveness, and the latter are less invasive and have larger electrode sites but have higher stimulation thresholds due to greater distance to target neurons. The challenge thus lies in the combination of minimally invasive, safe and efficient stimulation with small electrode sites and high spatial specificity. PEDOT:PSS was shown here to allow for the combination of safe and efficient stimulation with small electrode sites, therefore can be implemented to improve ABI functionality. Possible approaches to finely tune the stimulation characteristics include the adaptation of the stimulation waveform to the properties of the target neurons or current steering through careful selection of bipolar electrodes and inter-electrode distances. The use of PEDOT:PSS coatings on small electrode sites thus provides a tool for the optimization of the ABI array and stimulation protocol, which might lead to a better understanding of the functionality of current clinical ABI arrays and eventually to an improvement of speech hearing outcomes.

Acknowledgements

This work was supported by the Fondation Bertarelli and the National Institute of Health (grant DC01089).

References

1 C. Vincent, *Anatomical Rec.*, 2012, **295**, 1981–1986.
2 M. S. Schwartz, S. R. Otto, R. V. Shannon, W. E. Hitselberger and D. E. Brackmann, *Neurotherapeutics*, 2008, **5**, 128–136.
3 J. Subbaroyan, D. C. Martin and D. R. Kipke, *J. Neural. Eng.*, 2005, **2**, 103–113.
4 J. K. Nguyen, D. J. Park, J. L. Skousen, A. E. Hess-Dunning, D. J. Tyler, S. J. Rowan, C. Weder and J. R. Capadona, *J. Neural. Eng.*, 2014, **11**, 056014.
5 M. Asplund, T. Nyberg and O. Inganas, *Polym. Chem.*, 2010, **1**, 1374–1391.
6 X. Y. Cui and D. C. Martin, *Sens. Actuators, B*, 2003, **89**, 92–102.
7 X. T. Cui and D. D. Zhou, *IEEE Trans Neural Syst Rehabil Eng*, 2007, **15**, 502–508.
8 S. M. Richardson-Burns, J. L. Hendricks, B. Foster, L. K. Povlich, D.-H. Kim and D. C. Martin, *Biomaterials*, 2007, **28**, 1539–1552.
9 K. A. Ludwig, J. D. Uram, J. Y. Yang, D. C. Martin and D. R. Kipke, *J. Neural. Eng.*, 2006, **3**, 59–70.
10 L. Ouyang, C. L. Shaw, C.-C. Kuo, A. L. Griffin and D. C. Martin, *J. Neural. Eng.*, 2014, **11**, 026005.
11 J. A. Chikar, J. L. Hendricks, S. M. Richardson-Burns, Y. Raphael, B. E. Pfingst and D. C. Martin, *Biomaterials*, 2012, **33**, 1982–1990.
12 A. S. Koivuniemi and K. J. Otto, The depth, waveform and pulse rate for electrical microstimulation of the auditory cortex, *Proceedings of the 34th Annual International conference of the IEEE IMBS*, 2012, 2489–2492.
13 D.-H. Kim, J. a. Wiler, D. J. Anderson, D. R. Kipke and D. C. Martin, *Acta Biomater.*, 2010, **6**, 57–62.
14 R. A. Green, P. B. Matteucci, R. T. Hassarati, B. Giraud, C. W. Dodds, S. Chen, P. J. Byrnes-Preston, G. J. Suaning, L. A. Poole-Warren and N. H. Lovell, *J. Neural. Eng.*, 2013, **10**, 16009.
15 N. A. Shaw, *Prog. Neurobiol.*, 1988, **31**, 19–45.
16 A. Mercanzini, K. Cheung, D. L. Buhl, M. Boers, A. Maillard, P. Colin, J. C. Bensadoun, A. Bertsch and P. Renaud, *Sens. Actuators, A*, 2008, **143**, 90–96.
17 P. J. Rousche, D. S. Pellinen, D. P. Pivin, J. C. Williams, R. J. Vetter and D. R. Kipke, *IEEE Trans. Biomed. Eng.*, 2001, **48**, 361–371.
18 S. F. Cogan, P. R. Troyk, J. Ehrlich, T. D. Plante and D. E. Detlefsen, *IEEE Trans. Biomed. Eng.*, 2006, **53**, 327–332.
19 R. U. Verma, A. A. Guex, K. E. Hancock, N. Durakovic, C. M. McKay, M. C. C. Slama, M. C. Brown and D. J. Lee, *Hear. Res.*, 2014, **310**, 69–75.
20 D. H. Kim, J. Viventi, J. J. Amsden, J. L. Xiao, L. Vigeland, Y. S. Kim, J. A. Blanco, B. Panilaitis, E. S. Frechette, D. Contreras, D. L. Kaplan, F. G. Omenetto, Y. G. Huang, K. C. Hwang, M. R. Zakin, B. Litt and J. A. Rogers, *Nat. Mater.*, 2010, **9**, 511–517.
21 D. R. Merrill, M. Bikson and J. G. R. Jefferys, *J. Neurosci. Methods*, 2005, **141**, 171–198.
22 D. B. Mccreery, W. F. Agnew, T. G. H. Yuen and L. Bullara, *IEEE Trans. Biomed. Eng.*, 1990, **37**, 996–1001.
23 S. R. Otto, R. V. Shannon, E. P. Wilkinson, W. E. Hitselberger, D. B. Mccreery, J. K. Moore and D. E. Brackmann, *Otol. Neurotol.*, 2008, 1147–1154.